Laser-assisted surface defects and pore reduction of additive manufactured titanium parts

Zabihollah Ahmadi[1,2], Seungjong Lee[2,3], Nima Shamsaei[2,3*], Masoud Mahjouri-Samani[1,2*]

[1] Electrical and Computer Engineering Department, Auburn University, Auburn, AL, USA.

[2] National Center for Additive Manufacturing Excellence (NCAME), Auburn University, Auburn, AL, USA.

[3] Mechanical and Material Engineering Department, Auburn University, Auburn, AL, USA.

*Address correspondence to: mahjouri@auburn.edu, shamsaei@auburn.edu

Abstract

Laser surface treatment of additively manufactured parts has attracted considerable interest in the past few years due to its flexibility, operation speed, and capability for polishing complex surfaces as compared to conventional mechanical based methods. This study presents the role of laser surface processing in minimizing the surface roughness and pores that have detrimental effects on the fatigue behavior of additively manufactured specimens. This study is performed by a precise laser melting and recrystallization process to close the pores within 70 μm of the surface in order to enhance the fatigue life of these specimens. A continuous-wave fiber laser is employed to investigate the effect of various processing parameters for controlled laser surface treatments in this study.

1. Introduction

Titanium (Ti) alloys have wide use in various applications including aerospace, biomedical fields, chemical process equipment, nuclear reactor components, gears, missile fittings, and jet engine parts due to high specific strength and excellent corrosionresistance[1-3]. Conventional machinery manufacturing of titanium alloy components is challenging due to low thermal conductivity and high chemical reactivity with cutting tool materials[4-5]. Laser-based additive manufacturing (LBAM) of metallic parts such as laser beam powder bed fusion (LB-PBF) has

attracted much attention as a promising technology for producing titanium alloy parts using a layer-by-layer manufacturing process[6-7]. Such laser-based techniques have been commonly used for fabricating or repairing complex components including steam turbine blade, turbo-engine blade, and turbo-engine case[8-9]. The surface roughness of the LB-PBF parts is usually higher than 10 μm due to the nature of the fabrication process and layered structures[10-11].

Laser surface treatment is a potential method to reduce the surface roughness of additively manufactured (AM) parts through controlled laser-induced melting and recrystallization processes. When a laser beam with sufficient energy density irradiates on a material surface, the surface of material reaches the melting temperature and melt quickly due to fast photon-electron coupling and a subsequent electron-phonon energy transfer processes. After the formation of the molten pool, liquid material re-solidifies as the surface temperature drops behind the laser beam, resulting in the reduction of surface roughness for the right processing parameters [12-14]. Compared to conventional mechanical methods, laser surface treatment (LST) can offer a selective and localized processing ability with high automation in an environmental friendly approach. Also, LST has been considered as a promising method for polishing three-dimensional (3D) complex workpieces with less pollution and tools wear.

In recent decades, laser polishing processes have been developed for metallic materials, especially for metals that are difficult to machine. Chang et al. reported the surface polishing process of SKD61 tool steel using a microsecond pulsed fiber laser, and they reduced the surface roughness from 0.28 to 0.13 μm[15]. Using microsecond Nd:YAG laser, Guo et al. showed a reduction of roughness value from 0.4 to 0.12 μm of originally milled DF2 tool steel [16]. Giorleo et al. studied a polishing process executed with a Nd:YVO4 laser radiation on titanium sheet and the surface was polished from 0.58 to 0.42 μm. Laser macro polishing with a high-power laser has also been developed to adapt much more complex surfaces. Bordatchev et al. compared the polishing effect of CW and pulsed lasers on Ni alloy and reduced the surface roughness from 10 μm to 2 μm[17]. With the rise of AM technology, laser polishing has been used to finish AM parts surfaces.

Partially melted powders attached to the surface of the AM specimens may function as a region of high-stress concentrations and hence the locations for initiation of cracks. The surface finish of AM parts is much rougher than the machine part generated. This high level of surface roughness can severely impact the fatigue behavior of the AM parts. Optimizing laser parameters, improving

powder characteristics, performing machining of surface and applying post-heat treatments such as stress relieving and hot isostatic pressing are some of the common approaches to reduce the possibility of crack formation. Nezhadfar et al. studied five different heat treatment procedures for both as-build and machined surface conditions and reported that heat treatment procedures significantly increased the fatigue strength of 17-4 PH SS[24]. Although a large number of research activities has been conducted in improving fatigue life, however, there has not been many efforts in studying the effect of laser polishing and surface treatment on fatigue behavior of AM parts.

In this paper, we performed laser surface treatment on both as-built and heat-treated AM Ti6Al4V parts using a CW fiber laser (wavelength: 1064 nm). The objective of this study was to understand the effects of laser surface treatment on minimizing the surface roughness and hence improve their fatigue behavior. By analyzing the surface morphology, we discuss the laser treatment effects on the surface roughness of these titanium alloys. Figure 1 demonstrates the images of AM parts before and after the laser treatment process and the dimension of the specimen.

Figure 1. (a) Optical images of parts before (top) and after (bottom) the laser surface treatment. (b) Dimensions of the fabricated parts.

2. LST experimental setup

2.1. Materials

The specimens were fabricated by an EOS M290 LB-PBF AM machine. Titanium alloy LPW Ti-6Al-4V grade 23 powder by Carpenter Additive was used for fabricating these parts. The chemical composition of Ti64 powder is shown in Table 1. The design criteria of specimens for testing the fatigue behavior is based on American Society for Testing and Materials (ASTM) E606. EOS M290 was operated with default direct part parameters for Ti64: laser power of 280 W, scan speed of 1200 mm/s, hatch distance of 0.14mm and layer thickness of 40 μm. In addition, it went through a contouring process after scanning the part to decrease surface roughness. The build orientation was vertical to the plate and the steel blade was used as a recoater to scatter powder on

the build plate since it can provide more pressure to the powder during scattering. After the build was completed, the specimens were carefully detached from the substrate and stored separately to maintain the surface in as-built condition.

Element	Al	C	Fe	H	N	O	Ti	V	Res Total
Chemical Composition (wt %)	5.5 ~ 6.5	0.08	0.25	0.0125	0.03	0.13	Bal	3.5 ~ 4.5	0.4

Table 1. Chemical composition of Ti-6Al-4V powder produced by Carpenter Additive.

2.2. Laser Processing

Due to different absorptivity of metallic parts, for LST of specimens, two types of lasers (CW and Pulsed lasers) were employed to find suitable process parameters. The CW fiber laser was found to be more effective in reducing the surface roughness of the Ti parts in this study. The laser beam was coupled into a galvo scanner with a ~15 μm focal point and a scan speed ranging from 1 to 5000 $mm.s^{-1}$. A laser marking software (Laser Studio Professional) was used to design various patterns and control the process parameters (e.g., power, pulse duration, number of pulses, scan speed, repetition rate) for each specific pattern. The AM parts were installed on a rotary axis for controlled processing of the parts along the length of the cylindrical part as they rotate. To avoid surface oxidation during the LST process, experiments were performed in an argon environment within a costume-designed processing chamber. Figure 2 shows the designed experimental environment in this process. The influence of various parameters such as laser power (from 10W to 180W) and laser scanning speed (from 10mm/sec to 400mm/sec) was studied to find the optimized parameters. According to a large number of experiments, the optimized parameters for laser surface treatment were found to be 120W, 100 mm/s.

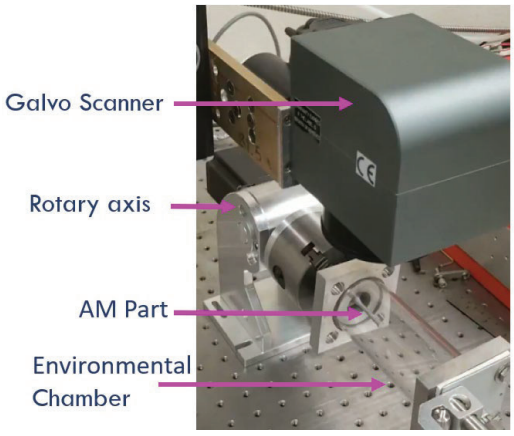

Figure 2. Experimental setup for laser surface treatment process.

2.3. Surface Roughness

The surface roughness of gage sections was investigated by a digital microscope (Keyence VHX-6000). Both as-built and laser-treated surface conditions were investigated. The direction of measurement was parallel to the build orientation to observe differences between layers as the roughness along build orientation is higher due to the layer-by-layer build process. To take large scan images at high magnifications, the 3D stitching was performed. The 3D stitching automatically handled various focal distances for each location and stitched images taken from various locations. From each image, we investigated not only five-line profiles to analyze roughness on the direction same as load direction but also area profiles to analyze 2D roughness on the surface. Figures 3 and 4 show the line and area profiles for surface roughness analysis obtained at 500X magnification.

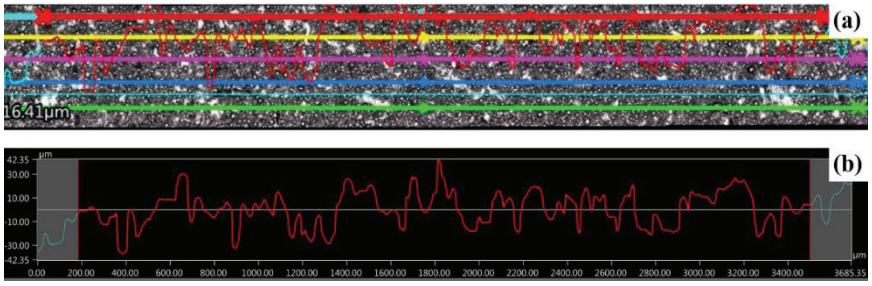

Figure 3. (a) Five profiled lines on the surface of gage section. (b) The topography of profiled line roughness. The centerline describes the average of profiled height values.

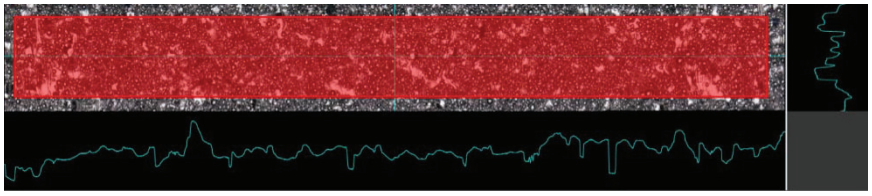

Figure 4. A 2D profile showing the surface topography of the samples.

3. Result and discussion

3.1. Laser surface treatment process parameters

The process parameters of the laser surface treatment were mainly found by a sequence of experimental investigations. The hatching space and focal distance were kept constant to simplify the process parameter space. Various laser power and laser scanning speed were then tested. Figure 5 shows different surface conditions produced by various process parameters. In addition, the

depth of the melt pool produced by the laser surface treatment was investigated as shown in figure 6. We observed that if the laser scan speed is too fast at constant power, the absorbed energy on the surface is not sufficient for melting the surface materials. Similarly, slow scan speed resulted in removing materials and creating deep trenches on the part surface. Upon extensive experimentation, a laser power of ~120W and laser scanning speed of 100mm/s was found to be optimized process parameters in this surface treatment study.

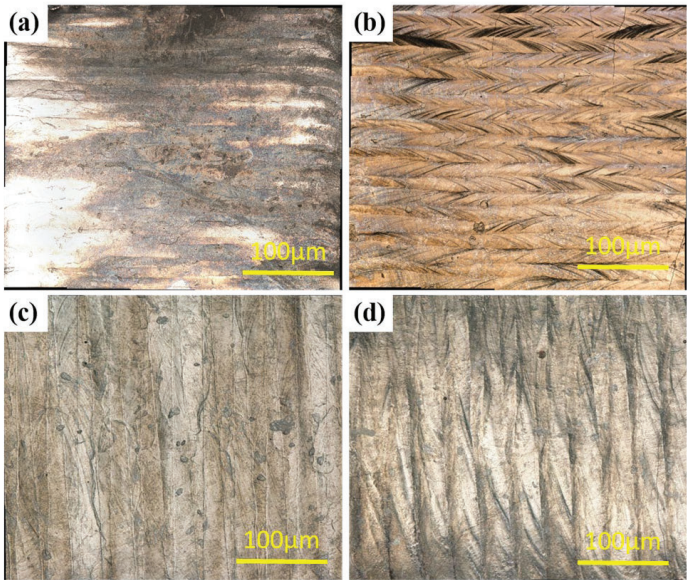

Figure 5. Surface conditions produced by various process parameters (laser powder and laser scanning speed). (a) 100W, 100mm/s. (b) 100W, 400mm/s. (c) 200W, 100mm/s. (d) 200W, 400mm/s.

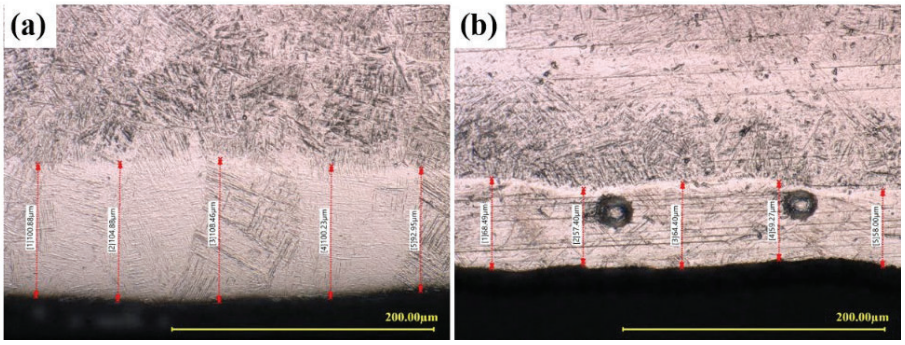

Figure 6. Depths of melt pool produced by different laser scanning speed. (a) 100W, 100mm/s. (b) 100W, 400mm/s

3.2.Effect of laser treatment on the surface morphology

A controlled melt pool was created by the incident laser beam. The laser beam was moved over the surface with a defined scanning velocity and power so that material was molten on one side of the melt pool and solidifies on the other side. Due to the surface tension of the molten material the surface roughness was smoothed during the melting process. The initial roughness of the samples before laser surface treatment was about 25 µm which were then reduced to below 5 µm after the laser processing. If the processing parameters were not well optimized and the inert environment was not fully maintained, some roughness and defects still remained on the final surface morphology that could be suitable sites for crack initiation and hence reducing the fatigue resistance.

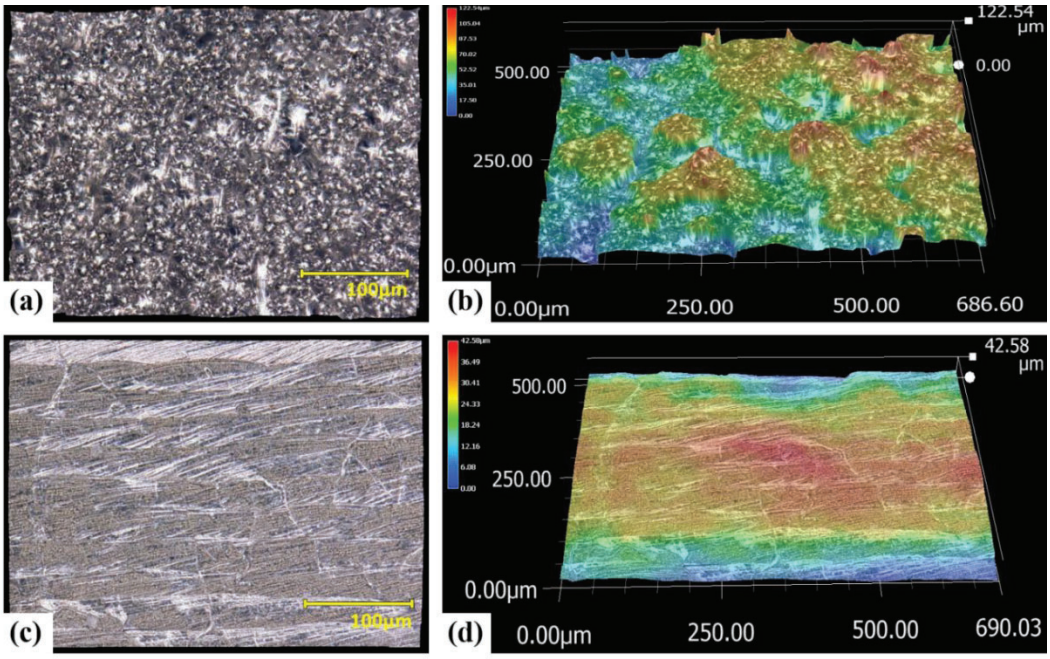

Figure 7. Surface topographies (a) and tilted 3D color map (b) of an as-built part. Surface topographies (c) and tilted 3D color map (d) of a laser-treated part.

Figure 7 shows the surface topographies of the Ti-6Al-4V samples before and after the laser surface treatment process under the optimized laser power and scanning speed. According to a large number of experiments, the optimized parameters for laser surface treatment were found to be 120W, 100 mm/s. The average melt pool depth using these parameters was reached 70 µm. As it is shown in figure 8, crystalline structure and grain boundaries were observed after optimum laser processing conditions.

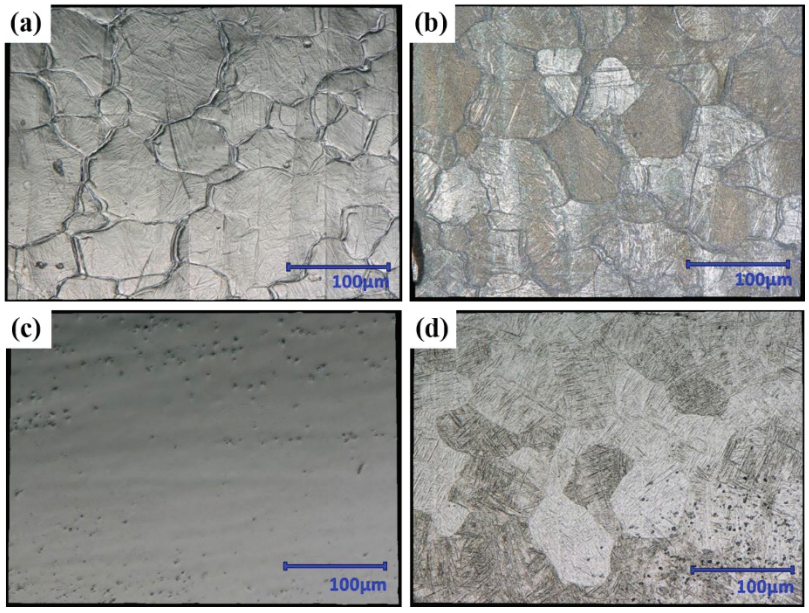

Figure 8. Optical images of the surface after the laser treatment, chemical etching, and polishing sequence. (a) as-laser-treated part, (b) chemically etched, (c) polished, (d) chemically etched again.

3.3. Improvement of surface roughness

There are representative parameters which describe surface roughness in one and two dimensions with numerical values including; (1) arithmetic media of all measured values on the profile (R_a, S_a), (2) maximum profile height (R_z, S_z), and (3) Japanese industrial standard for R_z (R_zJIS). In this study, arithmetical mean deviation represents the surface roughness as it is the most common and accurate value that calculates the entire profile. The average of five Ra from the five-line roughness and Sa from the area roughness provided the final surface roughness values. The Ra of as-built specimen was 13.27 μ m and Sa was 15.46 μ m, on the other hand, the Ra of the laser-treated specimen was 3.80 μ m and Sa was 4.15 μ m. Laser surface treatment process reduced ~70% of surface roughness on the loading direction. Rough surface conditions typically cause microcracks which exert a negative influence on fatigue behavior, especially in high cycle environments. In addition, the reduction of surface roughness in the direction perpendicular to the loading was verified by Sa change. In short, the surface condition was improved by laser treatment, hence improving the mechanical performance as observed from our current ongoing tests.

4. Conclusion

In the present paper, the laser surface treatment of AM Ti-6Al-4 specimens using a CW fiber laser was studied. This technique provided the ability to reduce the surface roughness of additive manufactured parts while allowing fine control over the structure of the surface materials as the melt and recrystallize during the process. This method, compared to the conventional methods, allows processing of complex surfaces without the need for further sample preparation at lower operation cost and at higher processing speed. The cyclic mechanical tests are currently under investigation which demonstrates noticeable improvement in their fatigue life.

1. Nouari, M.; Calamaz, M.; Girot, F., Wear mechanisms of cutting tools used in the dry machining of the aeronautic titanium alloy, Ti-6Al-4V. *Cr Mecanique* **2008,** *336* (10), 772-781.

2. Petersen, R. C., Titanium Implant Osseointegration Problems with Alternate Solutions Using Epoxy/Carbon-Fiber-Reinforced Composite. *Metals-Basel* **2014,** *4* (4), 549-569.

3. Qin, J. H.; Chen, Q.; Yang, C. Y.; Huang, Y., Research process on property and application of metal porous materials. *J Alloy Compd* **2016,** *654*, 39-44.

4. Pervaiz, S.; Rashid, A.; Deiab, I.; Nicolescu, M., Influence of Tool Materials on Machinability of Titanium- and Nickel-Based Alloys: A Review. *Mater Manuf Process* **2014,** *29* (3), 219-252.

5. Zhang, S.; Li, J. F.; Sun, J.; Jiang, F., Tool wear and cutting forces variation in high-speed end-milling Ti-6Al-4V alloy. *Int J Adv Manuf Tech* **2010,** *46* (1-4), 69-78.

6. Frazier, W. E., Metal Additive Manufacturing: A Review. *J Mater Eng Perform* **2014,** *23* (6), 1917-1928.

7. Basak, A.; Das, S., Epitaxy and Microstructure Evolution in Metal Additive Manufacturing. *Annu Rev Mater Res* **2016,** *46*, 125-149.

8. Lu, Z. L.; Zhang, A. F.; Tong, Z. Q.; Yang, X. H.; Li, D. C.; Lu, B. H., Fabricating the Steam Turbine Blade by Direct Laser Forming. *Mater Manuf Process* **2011,** *26* (7), 879-885.

9. Strano, G.; Hao, L.; Everson, R. M.; Evans, K. E., Surface roughness analysis, modelling and prediction in selective laser melting. *J Mater Process Tech* **2013,** *213* (4), 589-597.

10. Pakkanen, J.; Calignano, F.; Trevisan, F.; Lorusso, M.; Ambrosio, E. P.; Manfredi, D.; Fino, P., Study of Internal Channel Surface Roughnesses Manufactured by Selective Laser Melting in Aluminum and Titanium Alloys. *Metall Mater Trans A* **2016,** *47a* (8), 3837-3844.

11. Wang, M.; Lin, X.; Huang, W., Laser additive manufacture of titanium alloys. *Mater Technol* **2016,** *31* (2), 90-97.

12. Pfefferkorn, F. E.; Duffie, N. A.; Morrow, J. D.; Wang, Q. H., Effect of beam diameter on pulsed laser polishing of S7 tool steel. *Cirp Ann-Manuf Techn* **2014,** *63* (1), 237-240.

13. Ukar, E.; Lamikiz, A.; Liebana, F.; Martinez, S.; Tabernero, I., An industrial approach of laser polishing with different laser sources. *Materialwiss Werkst* **2015,** *46* (7), 661-667.

14. Wang, Q. H.; Morrow, J. D.; Ma, C.; Duffie, N. A.; Pfefferkorn, F. E., Surface prediction model for thermocapillary regime pulsed laser micro polishing of metals. *J Manuf Process* **2015,** *20*, 340-348.

15. Chang, C. S.; Chen, T. H.; Li, T. C.; Lin, S. L.; Liu, S. H.; Lin, J. F., Influence of laser beam fluence on surface quality, microstructure, mechanical properties, and tribological results for laser polishing of SKD61 tool steel. *J Mater Process Tech* **2016,** *229*, 22-35.

16. Guo, W.; Hua, M.; Tse, P. W. T.; Mok, A. C. K., Process parameters selection for laser polishing DF2 (AISI O1) by Nd:YAG pulsed laser using orthogonal design. *Int J Adv Manuf Tech* **2012,** *59* (9-12), 1009-1023.

17. Bordatchev, E. V.; Hafiz, A. M. K.; Tutunea-Fatan, O. R., Performance of laser polishing in finishing of metallic surfaces. *Int J Adv Manuf Tech* **2014,** *73* (1-4), 35-52.

18. Lamikiz, A.; Sanchez, J. A.; de Lacalle, L. N. L.; Arana, J. L., Laser polishing of parts built up by selective laser sintering. *Int J Mach Tool Manu* **2007,** *47* (12-13), 2040-2050.

20. J. Schmidt, R. Scholz, H. Riegel. Laser polishing of aluminum by remelting with high energy pulses. Materialwiss Werkst **2015**;46(7):686-691.

21. C.P. Ma, Y.C. Guan, W. Zhou. Laser polishing of additive manufactured Ti alloys. Opt Laser Eng **2017**;93:171-177.

22. E. Ukar, A. Lamikiz, L.N.L. de Lacalle, D. del Pozo, J.L. Arana. Laser polishing of tool steel with CO2 laser and high-power diode laser. Int J Mach Tool Manu **2010**;50(1):115-125.

23. D. Bhaduri, P. Penchev, A. Batal, S. Dimov, S.L. Soo, S. Sten, U. Harrysson, Z.X. Zhang, H.S. Dong. Laser polishing of 3D printed mesoscale components. Appl Surf Sci **2017**;405:29-46.

24. Nezhadfar, P. D., et al. "Fatigue behavior of additively manufactured 17-4 PH stainless steel: Synergistic effects of surface roughness and heat treatment." *International Journal of Fatigue* 124 (**2019**): 188-204.

25. S. Cheruvathur, E.A. Lass, C.E. Campbell, Additive manufacturing of 17-4 ph stainless steel: post-processing heat treatment to achieve uniform reproducible microstructure, JOM 68(3) (**2015**) 930-942.

26. M.R. Stoudt, R.E. Ricker, E. Lass, L.E. Levine, Influence of postbuild microstructure on the electrochemical behavior of additively manufactured 17-4 PH stainless steel, JOM 69(3) (**2017**)506-15.